Analytical Methods

Accepted Manuscript

This article can be cited before page numbers have been issued, to do this please use: K. Qin, R. Bai, X. Zhao, Y. Yang, X. Wang and L. Dong, *Anal. Methods*, 2025, DOI: 10.1039/D5AY01026H.

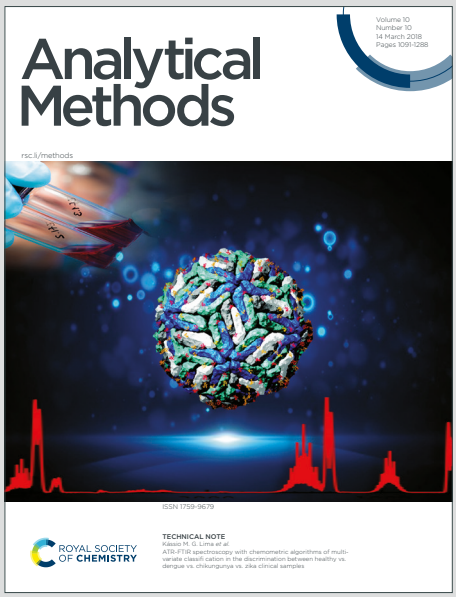

ROYAL SOCIETY OF CHEMISTRY

rsc.li/methods

View Article Online
DOI: 10.1039/D5AY01026H

ARTICLE

Dual-recognition fluorescent immunochromatographic strip based on IgG and antibiotic for smartphone-assisted detection of Staphylococcus aureus in food samples

Kai-Xin Qin [a,1] , Rui-Ting Bai [a,1] , Xiao-Xue Zhao [a,1], Yang Yang[a], Xian-Hua Wang [a]* , Lin-Yi Dong [a]*

Received 00th January 20xx,
Accepted 00th January 20xx

DOI: 10.1039/x0xx00000x

Staphylococcus aureus (*S. aureus)*, a bacterium ubiquitously distributed in natural environments and commonly colonizing human skin and mucous membranes, is a highly pathogenic agent that poses significant threats to human health. Consequently, the development of accurate and efficient detection methods for *S. aureus* is of utmost importance in clinical and public health contexts. Flow chromatography is widely used for the detection of *S. aureus* because of its short detection time and low demand for labor and material resources. Herein, we fabricated test strip sensors with dual recognition of IgG and cefradine (CE) for *S. aureus* detection, achieving a high degree of specificity and a low detection limit (10^2 CFU·mL^{-1}). Meanwhile, by capturing images of the T-line with a smartphone to quantify its fluorescence intensity, this method enabled both qualitative and quantitative detection of *S. aureus*. The detection process was simple, which required no personnel training, and takes only 40 minutes, offering fast and convenient analysis. To prove the practicability, we applied the test strip sensors to orange juice , milk and beef, and they were highly sensitive (orange juice: 10^2 CFU·mL^{-1}, milk: 10^4 CFU·mL^{-1}, beef: 10^4 CFU·mL^{-1}), reproducible (RSD<5.4%) .Therefore, we believe the test strip sensors have a bright application prospect in the field of rapid detection of *S. aureus*.

1. Introduction

Staphylococcus aureus (*S. aureus)* produces a variety of heat-stable enterotoxins that can persist even after cooking, thus ingestion of toxin-containing foods can lead to nausea, vomiting, and diarrhea. In immunocompromised individuals, inhalation of *S. aureus*-contaminated droplets may lead to fever, shortness of breath and even death. [1] In addition to this, skin infection with *S. aureus* can lead to bacteremia and a range of organ infections [2], such as osteomyelitis [3], pneumonia [4], and endocarditis[1]. *S. aureus* can be transmitted by contact and its presence is widespread, with a high probability of presence confirmed in hospitals and food farms[3, 5, 6] , therefore, the control of *S. aureus* is of great significance.

With advancements in technology, numerous methods for bacterial detection have been developed, including culture medium detection, immunoblotting[7], electrochemical detection[8,9], affinity molecular assay [10], recombinant enzyme polymerase amplification (RPA) [11], enzyme-linked immunosorbent assays (ELISA)[12], and lateral flow immunoassay [13-17], etc. Among these, LFIA stands out due to its efficiency. It requires minimal time, labor, and material resources, thus making it widely applicable for the detection of *S. aureus*.[18]However, it also has drawbacks, including high costs,

[a] *Tianjin Key Laboratory on Technologies Enabling Development of Clinical Therapeutics and Diagnostics, School of Pharmacy, Tianjin Medical University, Tianjin 300070, China.*
E-mail addresses: xianhua.w@163.com (X.-H. Wang), donglinyi@tmu.edu.cn (L.-Y. Dong) .

requiring professional instruments, and low sensitivities. To address these challenges, improving S. aureus detection via lateral flow chromatography remains crucial.

Specific recognition is the cornerstone of the test strip sensor. Currently, the detection of *S. aureus* mostly depends on the

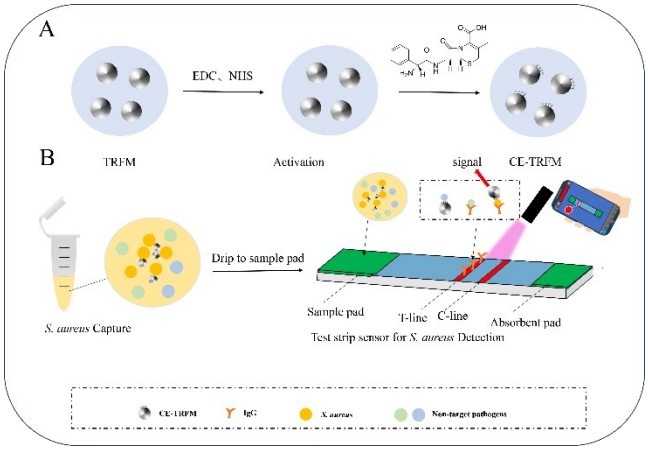

Scheme 1 A: Synthesis of CE-TRFM, B: LFIA test strips for detection of S. aureus

recognition of cis-diols by phenylboronic acid and its derivatives [19] or the capture of bacteria by antibodies [20] and aptamers [21]. However, phenylboronic acid and its derivatives exhibit very poor specificity for bacteria. While antibodies and aptamers have strong specificity, their production is time-consuming and costly. In addition, single-recognition systems are fundamentally limited by their cross-reactivity, as evidenced by two clinically significant cases. The Legionella urinary antigen EIA demonstrates this vulnerability, with false-positive rates reaching 39% due to antibody cross-reactivity with non-target pathogens like Pseudomonas aeruginosa and Enterobacteriaceae [22]. Similarly, Streptococcus pneumoniae antigen tests yield false positives due to the cross-reactivity of cell wall proteins in different streptococcal species [23]. These cases collectively demonstrate how single-target detection systems inherently risk misidentification due to structural similarities among bacterial antigens. To overcome these limitations, our dual-recognition strategy (IgG + CE) mitigates this risk by targeting both Protein A (IgG) and PBP2a (CE), thereby requiring two independent binding events for signal generation. The dual-recognition strategy combining CE and IgG offers a cost-effective and highly specific alternative (Scheme 1B), with advantages including easy availability, low cost, and high specificity, thereby lowering the technical barriers for *S. aureus* detection.

In addition to this, the signal output also determines the sensitivity of the test strip sensor. Common signal output molecules are colloidal gold[18], coloured microspheres, time-resolved fluorescent microspheres(TRFM), magnetic microspheres [15] and quantum dots. In order to ensure the stability of the signal output molecules and to improve the sensitivity of the detection, we used TRFM as the signal output. Specifically, we applied cefradine functionalized TRFM (CE-TRFM) combined with IgG for LFIA strips enabling rapid and cost-effective detection of *S. aureus*. The synthesized CE-TRFM could identify and capture *S. aureus*, so we could obtain *S. aureus*-CE-TRFM complex. When the *S. aureus*-CE-TRFM complex was added dropwise to the sample pad of the test strip sensor, the complex was specifically captured by IgG in the T-line. Meanwhile, the CE-TRFM uncaptured *S. aureus* continued to migrate along the test strip sensor and was captured by penicillin-binding proteins (PBPs) in the C-line. (Scheme1B). Under 365 nm excitation, CE-TRFM emitted red fluorescence, with signal intensity proportional to bacterial load. The fluorescence signal from the T-line was quantitatively analyzed using a smartphone by measuring the R-value in the RGB channels, which exhibited a linear correlation with the logarithmic bacterial concentration (102–108 CFU·mL^{-1}). The detection limit was 10^2 CFU·mL^{-1} by naked eye. In addition, test strip sensors were successfully performed in orange juice, milk and beef which were spiked with *S. aureus,* demonstrating the feasibility of this test strip sensor with recovery rates ranging from 89.04% to 108.90%, which is promising for the rapid detection of *S. aureus*.

2. Experimental Part

2.1. Materials ,reagents and instruments

Bovine serum albumin (BSA) was purchased from Shanghai Marel Biochemical Technology Co. Tween-20 was purchased from Tianjin Hynes Biochemical Technology Co. Human IgG dry powder, Phosphate buffer dry powder, *S. aureus*, *Escherichia coli O157:H7(E. ciol O157:H7)*, *Salmonella typhimurium*, *Listeria monocytogenes*, and *Candida albicans* were purchased from Beijing Soleilbao Science and Technology Co. 2-(N-morpholino)ethane sulfonic acid monohydrate (MES) was purchased from Shanghai Mclln Biochemical Science and Technology Co. 1-ethyl-(3-dimethylaminopropyl)carbodiimide (EDC) and N-hydroxy succinimide (NHS) were purchased from Shanghai Aladdin Biochemical Technology Co. CE and trichloroacetic acid (TCA) were purchased from Shanghai Ron Reagent. Sample pads, absorbent paper, and PVC base plate were purchased from Hangzhou Bluth Trading Co. NC membranes were purchased from Sartorius Scientific Instruments Co. TRFM were purchased from Tianjin Ena Micro Co.

The materials were synthesized using an electronic balance (Sartorius Scientific Instruments Co., Ltd.), pH meter PH3-3C (Yidian Scientific, Shanghai, China), ultrasonic cleaner KQ-3200B (Ultrasonic Instruments, Kunshan, China), and a high-speed centrifuge (Hunan Xiangyi Laboratory Instrument Development Co., Ltd.). The morphology and morphological structure of the synthesized materials were characterized by scanning electron microscopy (SEM, XL 30 ESEM, Philips, The Netherlands). The composition of the synthesized materials was investigated by Fourier Transform Infrared Spectrometer (FT-IR) (Nicolet 3800, Thermo Fisher, USA), Heat Loss Analyzer TG 209 F3 (Tarsus, Germany). Particle size and zeta potential of the prepared synthetic materials were recorded using Zetasizer Nano ZS90 (Malvern, UK). Fluorescence intensity of the prepared synthetics was recorded using fluorescence spectrophotometer F-7000 (Hitachi, Japan).

2.2. Bacterial culture

The microorganisms used in this study included *S. aureus*, *E. ciol O157:H7, Candida albicans*, *Listeria monocytogenes and Salmonella*

typhimurium. Firstly, 1 g of liquid medium was added to 40 mL of sterile water and dispersed well by sonication. Then, 2 μL of the strain was added and incubated in a water bath shaker at 37°C, 140 rpm for 10 h. Lastly, the bacterial solution was collected by centrifugation and diluted with phosphate buffered saline (PBS, 10mM, pH 7.4) to the test concentration.

2.3. Configuration of the solution

Activation buffer:195.24 mg MES was dissolved in 100 mL H_2O, and the pH was adjusted to 6.2 using 1 mol/L NaOH.

Coupling buffer:195.24 mg MES was dissolved in 100 mL H_2O, and the pH was adjusted to 5.0, 6.2, 7.4, 8.0, and 9.0 with 1 mol/L NaOH.

Microsphere closure solution:30.62 mg boric acid was dissolved in 100 mL H_2O to prepare a boric acid solution. Separately, 427.3 mg borax was dissolved in 100 mL H_2O to obtain a borax solution. The borax solution was slowly added to the boric acid solution, and the pH was adjusted to 9.0. After preparation, 20 mL was aliquoted, and 100 mg BSA and 10 mg Tween-20 were added.

Running buffer:100 mg BSA and 300 mg Tween-20 were added to 20 mL PBS solution.

2.4. Synthesis of CE-TRFM probe

The preparation steps of CE-TRFM were exhibited in Scheme 1A. Firstly,0.5 mg of TRFM was dispersed in 1 mL of activation buffer and then mixed with 3.5 μL of freshly prepared EDC solution (10 $mg{\cdot}mL^{-1}$), 33 μL of freshly prepared NHS solution (10 $mg{\cdot}mL^{-1}$)； after shaking at ambient temperature for 30 min，the activated TRFM was washed with 1.5 ml of coupling buffer. Subsequently, the activated TRFM was dispersed in 1 mL of coupling buffer and sonicated to disperse evenly, followed by adding 500 μL of CE (1 $mg{\cdot}mL^{-1}$); the mixed solution shook at ambient temperature for 2 h for antibiotic coupling. After shaking for 2 h, 1 mL of microsphere sealing solution was added, and shook at ambient temperature for 1 h. Finally, the synthetic CE-TRFM was washed with 1.5 mL of PBS, three times, and then stored in a refrigerator at 4°C with the concentration of 5 $mg{\cdot}mL^{-1}$.

2.5. Preparation of test strip sensors

The test strip sensor consisted of four components: sample pad, nitrocellulose filter membrane (NC membrane), absorbent pad, and polyvinyl chloride plates. All components were assembled onto polyvinyl chloride plates in an orderly manner, with an overlap of approximately 1-2 mm between two adjacent sections. Finally, the assembled test strip plates were cut into 2 mm widths and dried at 37°C for 12 h for further use.

2.6. Protein immobilization

In brief, 20 mL of *S. aureus* (OD_{600} of 1.0) was centrifuged at 6000 rpm for 10 min to remove the culture medium, followed by adding 400 μL of PBS buffer and 100 mg of grinding beads. Then mixture was vortexed for 20 min and centrifuged at 12,000 rpm for 15 min to remove the grinding beads and bacterial debris, yielding a supernatant containing the PBPs.

Lastly, 0.5 μL of PBPs was added at the C line of the test strip sensor, and 0.5 μL of 2.0 $mg{\cdot}mL^{-1}$ IgG was added at the T line, positioned 5 mm below the C line. The test strip sensors were placed in the oven at 37°C for 30 min. Fixed C- and T-line test strips can be stored for up to 2 weeks at 4°C under sealed dry conditions. The working temperature of test strips is room temperature.

2.7. Pre-treatment of food

The orange juice, milk and beef samples were purchased from local supermarket near to Tianjin Medical University and proved to be free from *S. aureus*. To prove the applicability, 4 mL of 3% TCA solution was added to 2 mL of orange juice and milk, respectively, and 3mL of 3% TCA solution was added to 1 g of beef. After centrifugation at 6000 rpm for 5 min, the precipitate was discarded, and the supernatant was taken. The treated orange juice and milk were adjusted to pH 7.4 with K_2CO_3 (0.1 M).[19] Finally,2 mL of each sample was mixed with 30 mg BSA and 90 mg Tween-20 to prepare the test sample buffer.

2.8. Test strip sensor procedure

S. aureus was centrifuged and resuspended in running buffer to obtain a concentration range of 0-10^8 $CFU{\cdot}mL^{-1}$. Next, 0.8 μL of CE-TRFM was added to 100 μL of bacterial solution and incubated for 30 min. Then, 30 μL of the mixture was added dropwise to the sample pad. After 10 min the results were photographed under 365 nm UV light. (Scheme 1B) If the sample contained *S. aureus*, the *S. aureus*-CE-TRFM complex was captured by IgG at the T-line, while, the unbound CE-TRFM was captured by the PBPs of the C-line. In this case, both the T-and Clines exhibited red fluorescence under 365 nm UV irradiation. Conversely, if the sample did not contain *S. aureus*, CE-TRFM was only captured by PBPs at the C line. This principle enabled qualitative detection of *S. aureus*. Quantitative detection of *S. aureus* was completed by analyzing high- quality photos using the Color Grab APP. The T line fluorescence intensity was quantified using the Color Grap software, with the extracted R-value of the serving as an indicator of the fluorescence strength.

To ensure the reproducibility of smartphone-based fluorescence quantification, all images were acquired under standardised conditions:

1. UV Illumination: A 365 nm UV lamp (6 watts) was fixed 23.5 cm perpendicular to the surface of the test strips.
2. Ambient Lighting: Images were taken in a dark room to eliminate ambient light interference.
3. Software analysis: The smartphone was fixed at the same height as the UV lamp to capture images. The Color Grab application (v3.9.2) was set to “Spot Metering” mode with the circular ROI (5mm diameter) centred on the T-line. In order to minimize the interference of the mobile phone model and the background signal of the NC membrane, the following quantitative approach was adopted to evaluate T-line fluorescence intensity and optimize experimental conditions.

$$\triangle R_{\text{negative/positive T line}} = R_{\text{T line}} - R_{\text{2mm above the T line}}$$

$$\triangle R = R_{\text{positive T line}} - R_{\text{negative T line}}$$

3. Results and discussion

3.1. Synthesis and characterization of CE-TRFM

View Article Online
DOI: 10.1039/D5AY01026H

ARTICLE

Table 1 Detailed information about TRFM

Name	Size（nm）	Potential（mv）	Carboxylic group content（μmol·g^{-1}）	Excitation wavelength（nm）	Emission wavelength（nm）
TRFM	307	-27	100	365	614

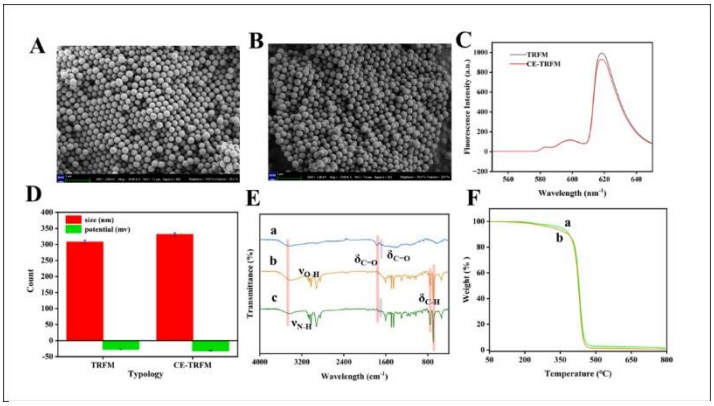

Fig. 1 A: SEM of TRFM, B: SEM of CE-TRFM, C: Fluorescence intensity of TRFM and CE-TRFM, D: Potential and particle size of TRFM and CE-TRFM, E: FT-IR spectroscopy of CE (a), TRFM (b), and CE-TRFM (c), F: TGA curves of TRFM (a) and CE-TRFM (b)

Detailed information of TRFM was showed in Table 1. AS shown in Fig. 1A and B, the morphology of TRFM remained unchanged and well-distributed before and after CE modification. Fig. 1C and D demonstrated that the fluorescence intensity of TRFM was largely unaffected by CE modification, while the absolute values of particle size and zeta potential slightly increased. Fourier transform infrared spectroscopy (FT-IR) and Thermogravimetric analysis (TGA) curves (Fig. 1E, F) confirmed the successful synthesis of CE-TRFM. The CE structure contained carboxyl and amide groups, with characteristic absorption peaks at 1773 cm^{-1} and 1685 cm^{-1} which were attributed to C=O vibrations. The very broad absorption peak at 3435 cm^{-1} was the peak of the stretching vibration of O-H. [24] For TRFM, the peaks at 697 cm^{-1} and 755 cm^{-1} corresponded to out-of-plane bending vibrations of hydrogen atoms on monosubstituted benzene rings , [25] while the absorption peak at 1760 cm^{-1} was attributed to C=O stretching of the carboxyl group in methacrylic acid, and the O-H stretching vibration appeared at 3435 cm^{-1} . [26]For CE-TRFM, the appearance of the C=O amide absorption peak at 1685 cm^{-1} (absent in TRFM) confirmed successful CE modification, while the N-H stretching vibration overlapped with the O-H stretching peak at 3435 cm^{-1} (Fig. 1E). Thermogravimetric analysis was performed to evaluate the mass loss of TRFM and CE-TRFM from 50°C to 800°C (Fig. 1F). CE exhibited a melting point of 140-142°C, and CE-TRFM demonstrated greater weight loss than TRFM between 140°C and 370°C, confirming the successful CE modification.

3.2. Recognizing the principle of molecule-specific capture of *S. aureus*

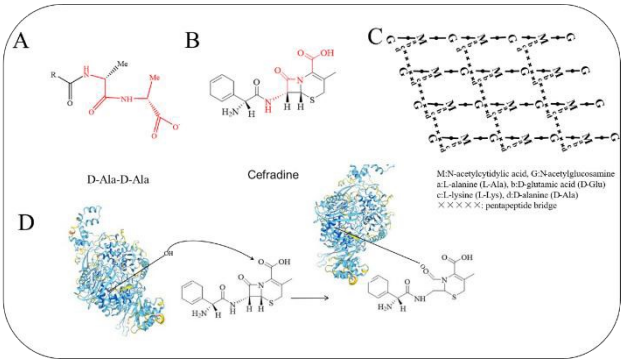

Scheme 2 Structural formula of the A tetrapeptide tail D-Ala-D-Ala and B CE, C: Structure of *S. aureus* peptidoglycan, D: Reaction mechanism of PBP with CE

The cross-linking of peptidoglycan peptide chains in *S. aureus* is catalyzed by PBPs. PBPs first attack the carbonyl group of the D-Ala-D-Ala peptide bond in the tetrapeptide tail, releasing a D-Ala molecule and exposing the reactive carboxylate group. The N-terminus of the glycine pentapeptide bridge binds to the carboxylate group of one tetrapeptide tail, while its C-terminus attaches to the ε-amino group of L-Lys in an adjacent tetrapeptide tail, forming a three-dimensional mesh structure (Scheme 2C) . [27] CE contains a D-Ala-D-Ala structure that mimics the PBPs' natural substrate (Scheme 2A, B). The serine residue (O^-) of PBPs attacks the β-lactam ring's carbonyl group, forming an irreversible acyl-enzyme intermediate that traps *S. aureus* (Scheme 2D). [28]

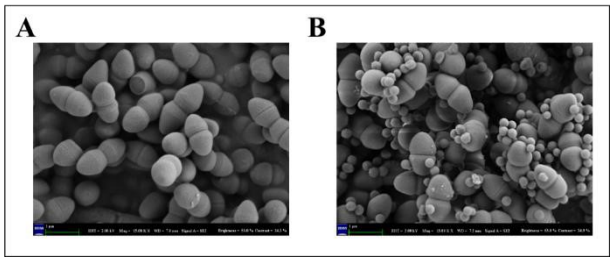

Fig. 2 A: SEM of *S. aureus*, B: SEM of CE-TRFM and *S. aureus*

To demonstrate that CE-TRFM could capture *S. aureus*, *S. aureus* alone and *S. aureus* mixed with CE-TRFM were observed separately under scanning electron microscopy (SEM). Many nanoscale spherical particles were found on the surface of S. aureus mixed with CE-TRFM, providing direct evidence of bacterial capture (Fig. 2A, B). In addition, IgG captured S. aureus primarily due to the widespread presence of staphylococcal protein A (SpA) on the bacterial surface, which contained specific binding sites for the Fc region of IgG. [29, 30]

CE was chosen over other β-lactams (including penicillin derivatives) because of its narrower antibacterial spectrum compared to other β-lactams and its bias towards Gram-positive bacteria, and its higher selectivity for *S. aureus*. CE has potent activity against Gram-positive bacteria (including *S. aureus*, *Streptococcus spp*, *S. pyogenes*, and *S. pneumoniae*), and is less potent against certain Gram-negative strains (such as *E. coli*, *K. pneumoniae*, *P. mirabilis*, and *Gonococcus*). [31] Meanwhile, the Fc region of IgG primarily binds to Protein A on *S. aureus* surfaces, but it also recognizes specific streptococcal antigens, including podoplanar polysaccharides and M proteins from *Group A hemolytic streptococci (GAS)*. [32]Although neither CE nor IgG targets S. aureus exclusively, their overlapping antimicrobial spectra are limited to *GAS*, *Streptococcus pneumoniae*, and *S. aureus*. However, *GAS* and *Streptococcus pneumoniae* cannot survive in food products, thus, dual screening with CE and IgG can specifically identify *S. aureus* in food.

3.3. Optimization of LFIA test strip sensor parameters for *S. aureus* detection

In order to obtain the LFIA test strip sensor with excellent fluorescence intensity, clear T-line, fast and accurate detection, the experiment optimized the pH of coupling buffer, the addition of CE and the pH of running buffer, the dosage of CE-TRFM probe, the incubation time, and the chromatography time. The pH of the coupling buffer and the amount of CE added both affect the ability of CE-TRFM to capture *S. aureus,* and therefore were optimized first. As shown in Fig. 3A, the ΔR values initially increased then decreased, reaching maximum intensity at pH 6.2, indicating optimal coupling efficiency between CE and TRFM at this pH. In the range of pH 5.0-6.2, with the increase of pH, the carboxyl group deprotonation (-COO-) was enhanced, the electrostatic repulsion was weakened, and the coupling efficiency was significantly increased; while in the range of pH 7.0-9.0, the hydrolysis of EDC and NHS was accelerated, and the β-lactam ring of CE also began to hydrolyse which led to the decrease of coupling efficiency and bacterial trapping ability. Therefore, the best coupling efficiency between CE and TRFM was achieved at pH 6.2. As shown in Fig. 3B, the ΔR initially increased then stabilized with increasing CE dosage. To conserve reagents, 0.5 mg CE was selected as the optimal amount. Next the parameters of the test strip sensor were optimized. The pH of the running buffer significantly affects the specific binding of the fluorescent probe to S. aureus and the non-specific adsorption of CE-TRFM to IgG. Under acidic conditions, there is electrostatic adsorption between the net positive charge present on the surface of IgG and the negatively charged CE-TRFM, resulting in strong non-specific adsorption (high R-negative values). Under neutral and alkaline conditions, the IgG surface was uncharged or negatively charged and the electrostatic adsorption disappeared. In addition, the CE structure is stable under neutral and acidic conditions, and under alkaline conditions the CE hydrolyses and has a reduced ability to capture bacteria. Therefore, pH 7.4 was selected as optimal (Fig. 3C). The CE-TRFM probe volume significantly impacted LFIA performance. From 0.2-0.8 μL, increasing probe volume enhanced IgG-captured complexes and ΔR values. However, from 0.8-1.4 μL, NC membrane background interference dominated (increased R-negativity), reducing ΔR. Thus, 0.8 μL was determined as the optimal probe volume (Fig. 3D). Finally, incubation and chromatography times were optimized. As time increased, *S. aureus* binding reached saturation, with ΔR peaking at 30 min incubation and 10 min running time before stabilizing (Fig.3E, F). The final optimized parameters were:

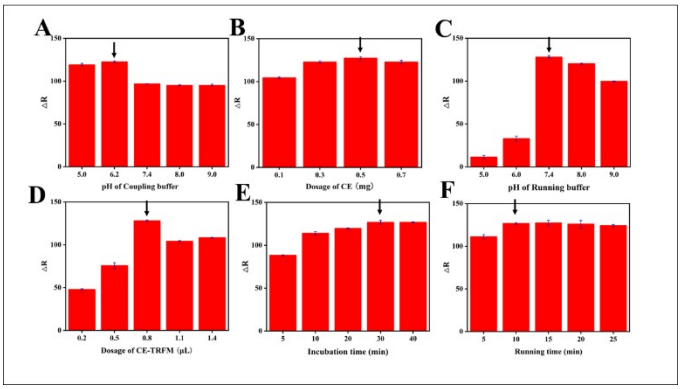

Fig. 3 Effect of A coupling buffer pH, B CE addition, C running buffer pH, D probe addition, E incubation time and running time

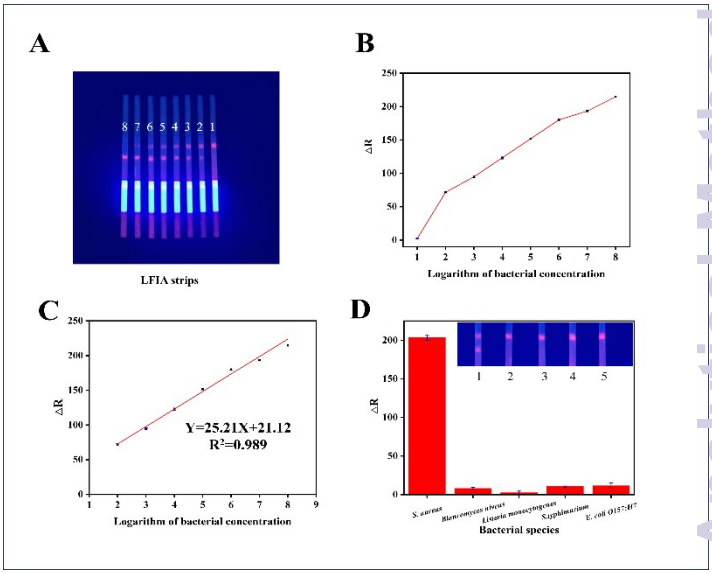

Fig. 4 A: Photographs of eight test strip sensors exposed to different *S. aureus* concentrations (10^1 to 10^8 CFU·mL^{-1}, right to left), B: Linear correlation between the logarithm of bacterial concentration and ΔR, C: Linear regression analysis between the logarithm of bacterial concentration and ΔR,D: Specificity testing with pathogens (in the photographs of the test strips, from left to right: *S. aureus*, *Candida albicans*, *Listeria monocytogenes*, *Salmonella typhimurium*, and *E. coli O157:H7*)

View Article Online DOI: 10.1039/D5AY01026J

coupling buffer pH 6.2, 0.5 mg CE, running buffer pH 7.4, 0.8 μL CE-TRFM probe, with 30 min incubation and 10 min running time.

3.4. Detection performance of LFIA test paper sensor for *S. aureus* detection

Based on the optimized conditions, we evaluated the detection range and sensitivity of the LFIA test strip sensor. *S. aureus* cultures were centrifuged at 6000 rpm for 10 min, resuspended in running buffer, and serially diluted to concentrations of 0, 10^1, 10^2, 10^3, 10^4, 10^5, 10^6, 10^7, and 10^8 CFU·mL^{-1}. These samples were incubated with the CE-TRFM probe and tested using the test strip sensors (Fig. 4A). The T line of negative samples showed only background signal from the NC membrane without detectable fluorescence. In positive samples, the fluorescence signal intensity increased proportionally with bacterial concentration, with a visual detection limit of 10^2 CFU·mL^{-1}. Using Color Grap smartphone software for quantification, we established a standard curve (ΔR vs. log S. aureus concentration) spanning 10^2-10^8 CFU·mL^{-1}, described by the equation Y = 25.21X + 21.12 (R^2 = 0.989) (Fig. 4B, C). To verify the specificity of the LFIA test strip sensor for *S. aureus* detection, we tested it against several common pathogens, including *Candida albicans*, *Listeria monocytogenes*, *Salmonella typhimurium*, and *E. coli O157:H7*. Bacterial suspensions (10^8 CFU·mL^{-1}) were prepared following the Bacterial culture method described in the experimental section. After incubating with the probes, the test strip sensors were run according to the assay procedure. As shown in Fig. 4D, the LFIA test strip sensor exhibited strong specificity for *S. aureus* with minimal cross-reactivity. To demonstrate the stability of the assay, we also performed an inter-day precision test (92.17%-114.80%, RSD<4.1%) and a multi-operator inter-precision test (92.17%-112.81, RSD<4.8%), as detailed in Table S1 and S2 of the Supplementary Material.

We compared this method with other S. aureus detection assays and found it to exhibit the highest sensitivity among flow-through chromatography-based techniques. Relative to alternative approaches, our method is cost-effective, rapid, and compatible with smartphone-based readout, facilitating widespread adoption for S. aureus detection (Table 2). The full names and brief explanations of the methods for detecting Staphylococcus aureus in Table 2 are detailed in Table S3 of the Supplementary Information.

Table 2 Detection of S. aureus

Recognition unit	Signal generator/ Analysis method	Limit of Detection (LOD)	Sample	detection time	ease-of-use (Specialised instruments and operators with highly sophisticated professional training are or are not required)	Ref
Primer	HAMP	86 CFU·mL^{-1}	Milk	1.25 h	easiness	33
Primer and CRISPR·Cas12a crRNA	ICS and fluorescence detection	LAMP-CRISPR/Cas12a-ICS platform：6.7*10^3 CFU·mL^{-1} RPA-CRISPR/Cas12a-flu platform:67 CFU·mL^{-1}	Pure bacterial culture	40 min	easiness	34
Staphylococcus aureus antibody	Fluorescent labeling method	15 CFU·μL^{-1}	Drinking water	1.5 h	difficulty	35
Dual Antibody (LTA+SPA)	Double Recognition CRISPR /Cas12a System	50 CFU·mL^{-1}	Serum, cell lysate	6 h	difficulty	36
Recombinant anti-Staphylococcus aureus antibody	FLISA/fluorescent labeling assay	3.1*10^6 CFU·mL^{-1}	Pure bacterial culture	5.3 h	difficulty	37
Nanoantibodies	ELISA/HRP-TMB color development system	1.4*10^5 CFU·mL^{-1}	Milk	Not mentioned in the paper	difficulty	38
Phage and IgG antibodies	Enzyme-catalyzed color development	PBS：2.47*10^3 CFU·mL^{-1} Apple juice：8.86*10^3 CFU·mL^{-1}	PBS、Apple juice	1.5 h	difficulty	39
Antibiotic and	RCA/fluorescent signal	3.3*10^2 CFU·mL^{-1}	Juice	1 h	difficulty	40

View Article Online
DOI: 10.1039/D5AY01026H

biotinylated IgG antibody Fluorescently labeled antibody	FCM/fluorescent signal	Milk：7.50 cells·mL^{-1} Powdered milk：8.30 cells·mL^{-1}	Milk、Powdered milk	6 h	difficulty	41
Primer	SSEA	Pork：1.0*10^{2} CFU·g^{-1} Duck or Scallop：1.0*10^{3} CFU·g^{-1}	Pork、Duck、Scallop	1 h	difficulty	42
Antibiotic	CD@Van/ fluorescent signal	3.18×10^{5}CFU·mL^{-1}	Orange juice	50 min	difficulty	43
Antibiotics and IgG	TRFM/LIFA	PBS:10^{2} CFU·mL^{-1} Orange juice：10^{2} CFU·mL^{-1} Milk：10^{4} CFU·mL^{-1}	PBS、Orange juice、Milk	40 min	easiness	This work

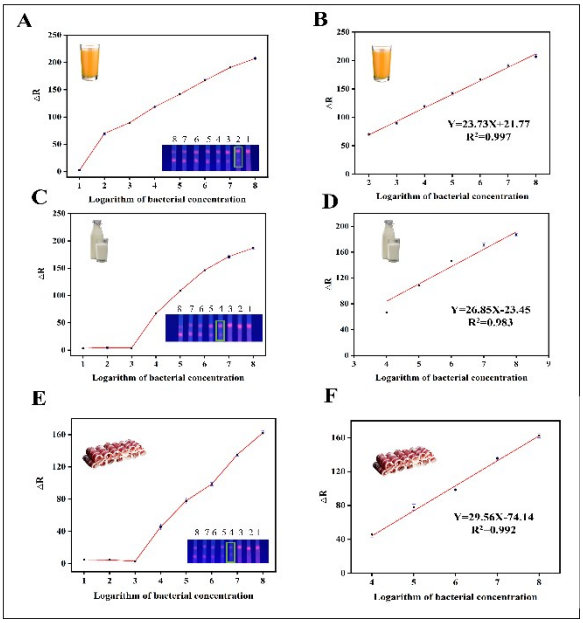

Fig. 5 Detection of S. aureus in different samples including orange juice (A, B),milk (C, D) and beef (E, F) using test strip sensors, with the logarithm of S. aureus concentration on top of the test strip

3.5.Detection of *S. aureus* in samples by LFIA test strip sensors

The *S. aureus* suspension was centrifuged at 6000 rpm for 10 min, resuspended in pre-treated test sample buffers., and serially diluted to concentrations ranging from 0 to 10^8 CFU·mL^{-1}, which were then incubated with the CE-TRFM probe for test strip senor analysis. In Orange juice samples, *S. aureus* concentrations demonstrated excellent linearity (Y=23.73X+21.77, R^2=0.997) across 10^2-10^8 CFU·mL^{-1} (Fig. 5A, B). The recovery rates for spiked samples (10^2, 10^4, 10^6, and 10^8 CFU·mL^{-1}) analyzed by LFIA test strips ranged from 97.57% to 108.75%, with RSD values of 2.0%-2.8% (Table 3), yielding an LOD of 10^2 CFU·mL^{-1}. For milk samples, *S. aureus* concentrations displayed good linearity (Y=26.85X-23.45, R^2=0.983) from 10^4-10^8 CFU·mL^{-1} (Fig. 5C, D). LFIA test strip analysis of spiked samples (10^4, 10^6, and 10^8 CFU·mL^{-1}) showed recovery rates of 89.04%-106.56% with RSDs of 2.5%-5.4% (Table 3), achieving an LOD of 10^4 CFU·mL^{-1}. For beef samples, *S. aureus* concentrations displayed good linearity (Y=29.56X-74.14, R^2=0.992) from 10^4-10^8 CFU·mL^{-1} (Fig. 5E,F). LFIA test strip analysis of spiked samples (10^4, 10^6, and 10^8 CFU·mL^{-1}) showed recovery rates of 95.69%-108.90% with RSDs of 3.6%-4.1% (Table 3), achieving an LOD of 10^4 CFU·mL^{-1}.

Table 3 Spiked recovery assay for Staphylococcus aureus in LFIA test strip assay

Sample	Spiked (log CFU·mL^{-1})	Found (log CFU·mL^{-1})	Recovery (%)	RSD（%，n=9）
Orange juice	2	2.09	104.67	2.8
	4	4.19	104.66	2.8
	6	6.17	102.86	2.5
	8	8.07	100.85	2.0

View Article Online DOI: 10.1039/D5AY01026H

Milk	4	3.91	97.87	5.4
	6	5.70	95.04	3.3
	8	7.71	96.37	2.5
Beef	4	3.96	99.07	3.7
	6	6.18	102.95	4.1
	8	8.10	101.22	3.6

Conclusions

In this study, we developed an LFIA test strip sensor for detecting *S. aureus* and successfully applied it to analyze orange juice, milk and beef samples spiked with *S. aureus*. The dual screening approach combining IgG and CE addressed the limitations of traditional antibody-based methods, including high cost and lengthy preparation time, while maintaining high specificity for *S. aureus*. The detection process requires no specialized training and can be completed within 40 minutes, offering rapid and convenient analysis. Using Color Grap software for data processing further enhances the test strip's potential for widespread adoption. The visual detection limit reached 10^2 CFU·mL^{-1}. When applied to orange juice, milk and beef samples spiked with *S. aureus*, the method demonstrated high sensitivity (orange juice: 10^2 CFU·mL^{-1}; milk: 10^4 CFU·mL^{-1}, beef: 10^4 CFU·mL^{-1}) and excellent reproducibility (RSD < 5.4%). With its rapid detection time and low cost, this method shows promising application prospects for lowering the technical barriers of *S. aureus* detection.

Author contributions

Kai-Xin Qin: Writing–original draft, Methodology. Investigation. Rui-Ting Bai: Writing–original draft, Methodology. Xiao-Xue Zhao: Formal analysis, Data curation. Yang Yang: Resources, Data curation. Lin-Yi Dong: Writing–review & editing, Methodology, Funding acquisition, Data curation. Xian Hua Wang: Methodology, Data curation, Conceptualization.

Conflicts of interest

The authors declare that they have no known competing financial interests or personal relationships that could have appeared to influence the work reported in this paper.

Data availability

All data supporting the findings of this study are available within the paper.

Acknowledgements

This work was financially supported by the National Natural Science Foundation of China (Grant No. 21605114) and Science & Technology Development Fund of Tianjin Education Commission for Higher Education (No. 2022ZD053).

Supporting information

Supplementary data associated with this article can be found in the online version.

References

1. B. A. Mengistu, K. Getnet, A. S. Mebratu and M. D. Fenta, *Frontiers in public health*, 2024, **12**, 1403012.
2. D. P. R. Troeman, D. Hazard, C. H. W. van Werkhoven, L. Timbermont, S. Malhotra-Kumar, M. Wolkewitz, A. Ruzin, F. Sifakis, S. Harbarth and J. Kluytmans, *Open forum infectious diseases*, 2024, **11**, ofae414.
3. A. H. Thaha, R. Malaka, W. Hatta and F. Maruddin, *Italian journal of food safety*, 2024, **13**, 12409.
4. S. Bae, M. S. Kook, E. Chang, J. Jung, M. J. Kim, Y. P. Chong, S. H. Kim, S. H. Choi, S. O. Lee and Y. S. Kim, *Open forum infectious diseases*, 2025, **12**, ofae734.
5. D. M. Alkuraythi and M. M. Alkhulaifi, *Veterinary world*,

2024, **17**, 1753-1764.
6. V. B. Mantovam, D. F. Dos Santos, L. C. Giola Junior, M. Landgraf, U. M. Pinto and S. D. Todorov, *Foodborne pathogens and disease*, 2025, DOI: 10.1089/fpd.2024.0124.
7. S. A. Zaidi, *Critical reviews in analytical chemistry*, 2021, **51**, 609-618.
8. A. K. Shukla, D. Park and B. Kim, *Analytica chimica acta*, 2024, **1319**, 342964.
9. M. M. El-Wekil, H. M. Halby, M. Darweesh, M. E. Ali and R. Ali, *Scientific reports*, 2022, **12**, 12502.
10. S. Shen, W. Wang, Y. Ma, S. Wang, S. Zhang, X. Cai, L. Chen, J. Zhang, Y. Li, X. Wu, J. Wei, Y. Zhao, A. Huang, S. Niu and D. Wang, *Nature communications*, 2024, **15**, 9304.
11. Y. Xing, C. Fan and J. Liu, *Clinical laboratory*, 2024, **70**.
12. S. C. Martins, C. A. Tararam, L. O. Levy, T. Arai, A. Watanabe, M. L. Moretti and P. Trabasso, *The Brazilian journal of infectious diseases : an official publication of the Brazilian Society of Infectious Diseases*, 2024, **28**, 103838.
13. P. Phothaworn, C. Meethai, W. Sirisarn and J. Y. Nale, *Viruses*, 2024, **16**.
14. M. C. Castañeda-Torres, J. Arango, A. Zuluaga, Á. Rúa-Giraldo and D. H. Caceres, *Medical mycology*, 2024, **63**.
15. C. Y. Wen, L. J. Zhao, Y. Wang, K. Wang, H. W. Li, X. Li, M. Zi and J. B. Zeng, *Mikrochimica acta*, 2023, **190**, 57.
16. H. Qi, Q. Sun, Y. Ma, P. Wu and J. Wang, *Toxins*, 2020, **12**.
17. J. Gao, Y. Jiao, J. Zhou and H. Zhang, *Talanta*, 2024, **270**, 125553.
18. K. Fujiuchi, N. Aoki, T. Ohtake, T. Iwashita and H. Kawasaki, *Biomedicines*, 2024, **12**.
19. P. Wu, F. Xue, W. Zuo, J. Yang, X. Liu, H. Jiang, J. Dai and Y. Ju, *Analytical chemistry*, 2022, **94**, 4277-4285.
20. S. Wiriyachaiporn, P. H. Howarth, K. D. Bruce and L. A. Dailey, *Diagnostic microbiology and infectious disease*, 2013, **75**, 28-36.
21. Z. Liu, L. Ji, Y. Li, X. Cao, X. Shao, J. Xia and Z. Wang, *Talanta*, 2024, **279**, 126655.
22. J. Como, M. A. Moffa, N. Bhanot, Z. Min, K. S. Cole, J. Kuzyck and T. L. Walsh, *European journal of clinical microbiology & infectious diseases : official publication of the European Society of Clinical Microbiology*, 2019, **38**, 1377-1382.
23. D. O. Shumway, K. Kriege and S. T. Wood, *Cureus*, 2023, **15**, e37458.
24. A. Khan, H. Jabeen, T. Ahmad, N. U. Rehman, S. S. Khan, H. Shareef, R. Sarwar, S. Yahya, N. Hussain, J. Uddin, J. Hussain and A. Al-Harrasi, *Artificial cells, nanomedicine, and biotechnology*, 2022, **50**, 312-321.
25. X. Teng, X. Ding, Z. She, Y. Li and X. Xiong, *Polymers*, 2022, **15**.
26. C. Zhang, Z. Zhang and Y. Qi, *Polymers*, 2021, **13**.
27. D. J. Waxman and J. L. Strominger, *Annual review of biochemistry*, 1983, **52**, 825-869.
28. D. Kim, S. Kim, Y. Kwon, Y. Kim, H. Park, K. Kwak, H. Lee, J. H. Lee, K. M. Jang, D. Kim, S. H. Lee and L. W. Kang, *Biomolecules & therapeutics*, 2023, **31**, 141-147.
29. S. Nandy, V. M. Maranholkar, M. Crum, K. Wasden, U. Patil, A. Goyal, B. Vu, K. Kourentzi, W. Mo, A. Henrickson, B. Demeler, M. Sen and R. C. Willson, *International journal of molecular sciences*, 2023, **24**.
30. X. Chen, O. Schneewind and D. Missiakas, *Proceedings of the National Academy of Sciences of the United States of America*, 2022, **119**.
31. L. M. Lima, B. Silva, G. Barbosa and E. J. Barreiro, *European journal of medicinal chemistry*, 2020, **208**, 112829.
32. V. Kumra Ahnlide, T. de Neergaard, M. Sundwall, T. Ambjörnsson and P. Nordenfelt, *Frontiers in immunology*, 2021, **12**, 629103.
33. A. A. P. Milton, M. C. B. Prasad, G. B. Priya, K. M. Momin, V. Lyngdoh, K. Srinivas, S. Das and S. Ghatak, *World journal of microbiology & biotechnology*, 2023, **40**, 14.
34. D. Xu, H. Zeng, W. Wu, H. Liu and J. Wang, *Foods (Basel, Switzerland)*, 2023, **12**.
35. B. Song, J. Wang, Z. Yan, Z. Liu, X. Pan, Y. Zhang and X. Zhang, *Bioengineered*, 2020, **11**, 1137-1145.
36. J. Yang, Y. Zhao, L. Qian, Y. Yu, Y. Zhang and J. Zhang, *Journal of hazardous materials*, 2024, **476**, 134877.
37. J. K. Kim, H. Y. Yun, J. S. Kim, W. Kim, C. S. Lee, B. G. Kim and H. J. Jeong, *Applied microbiology and biotechnology*, 2024, **108**, 2.
38. Y. Hu, Y. Sun, J. Gu, F. Yang, S. Wu, C. Zhang, X. Ji, H. Lv, S. Muyldermans and S. Wang, *Food chemistry*, 2021, **353**, 129481.
39. C. Yan, Y. Zhang, H. Yang, J. Yu and H. Wei, *Talanta*, 2017, **170**, 291-297.
40. Y. Wang, Z. Wang, Z. Zhan, J. Liu, T. Deng and H. Xu, *Analytica chimica acta*, 2022, **1189**, 339213.
41. S. Liu, B. Wang, Z. Sui, Z. Wang, L. Li, X. Zhen, W. Zhao and G. Zhou, *Foodborne pathogens and disease*, 2021, **18**, 346-353.
42. J. Zhang, X. Han, Y. Wang, X. Mu, C. Shi, Y. Li and C. Ma, *The Analyst*, 2023, **148**, 1970-1977.
43. D. Zhong, Y. Zhuo, Y. Feng and X. Yang, *Biosensors & bioelectronics*, 2015, **74**, 546-553.

All data supporting the findings of this study are available within the paper.

View Article Online
DOI: 10.1039/D5AY01026H